MODEL OF CALCIUM MOVEMENTS DURING ACTIVATION IN THE SARCOMERE OF FROG SKELETAL MUSCLE

M. B. CANNELL AND D. G. ALLEN
Department of Physiology, University College London, London WC1E 6BT, England

ABSTRACT A model of calcium movement during activation of frog skeletal muscle is described. The model was based on the half sarcomere of a myofibril and included compartments representing the terminal cisternae, the longitudinal sarcoplasmic reticulum, the extramyofibrillar space, and the myofibrillar space. The calcium-binding proteins troponin, parvalbumin, and calsequestrin were present in appropriate locations and with realistic binding kinetics. During activation a time-dependent permeability in the terminal cisternal wall led to calcium release into the myoplasm and its diffusion through the myoplasm longitudinally and radially was computed. After adjustment of three parameters, the model produced a myoplasmic free-calcium concentration that was very similar to those recorded experimentally with calcium indicators. The model has been used (*a*) to demonstrate the importance of parvalbumin in the relaxation of skeletal muscle, (*b*) to describe the time course and magnitude of calcium gradients associated with diffusion across the sarcomere, and (*c*) to estimate the errors associated with the use of aequorin as an intracellular calcium indicator in muscle.

INTRODUCTION

The development of tension in skeletal muscle involves the release of stored calcium from the terminal cisternae of the sarcoplasmic reticulum (SR) and the diffusion of calcium across the sarcomere to the troponin binding sites (Winegrad, 1968; Somlyo et al., 1981). Relaxation is brought about by the uptake of calcium by the SR (MacLennan and Holland, 1975), perhaps aided by myoplasmic calcium buffers (Gillis et al., 1982). The movement of calcium from release sites to binding sites and then back to uptake sites occurs by diffusion and involves the presence of gradients of calcium across the sarcomere. The magnitude and time course of these calcium gradients have not been measured because current methods of measuring myoplasmic free-calcium concentration (myoplasmic $[Ca^{2+}]$) do not have sufficient temporal or spatial resolution (Blinks et al., 1982). Calculation of the gradients is complicated by the geometry of the sarcomere and by the presence of various classes of calcium binding sites throughout the myoplasm.

The most important calcium-binding proteins in skeletal muscle are troponin, parvalbumin, and calsequestrin. Troponin is attached to the thin filaments, and binding of calcium to troponin leads to structural changes in a neighboring protein, tropomyosin, and allows actin and myosin interaction, which leads to tension production (Ebashi et al., 1969; Potter and Gergely, 1975). Parvalbumin is a soluble protein found in high concentration in the myoplasm of some muscles. Its function is uncertain, but Gillis et al. (1982) have suggested that it may increase the rate of relaxation. Calsequestrin is a low-affinity but high-capacity calcium-binding protein that is localized in the terminal cisternae (Jorgensen et al., 1979), and allows large amounts of calcium to be stored at this site without an excessively high $[Ca^{2+}]$.

We have developed a mathematical model that simulates the diffusion of calcium through the sarcomere. The model has been used for the following purposes: (*a*) to explore the intracellular mechanisms that lead to the measured myoplasmic $[Ca^{2+}]$ under various experimental conditions (in particular we consider the response to a single stimulus [twitch], the response to rapid series of stimuli [tetanus], and the rate of fall of myoplasmic $[Ca^{2+}]$ during relaxation from twitches and tetani), (*b*) to calculate the magnitude and time course of the myoplasmic $[Ca^{2+}]$ gradients across the sarcomere during activation and relaxation, and (*c*) to estimate the errors in the measurement of myoplasmic $[Ca^{2+}]$ that arise when aequorin is used as a calcium indicator in muscle.

Aequorin has been widely used as an intracellular calcium indicator in skeletal and cardiac muscle because of its sensitivity and relative immunity to movement artifacts (for review see Blinks et al., 1982). However, the relation between light (L) and $[Ca^{2+}]$ is nonlinear with $L \propto [Ca^{2+}]^{2.5}$ in the physiological range (Allen et al., 1977). Consequently, when there are gradients of calcium present, areas with a high $[Ca^{2+}]$ produce very large light signals. Thus, when light from the whole preparation is collected (spatial averaging), the resulting light signal is not proportional to the mean $[Ca^{2+}]$ across the preparation (Baker et

Dr. Cannell's present address is the Department of Physiology, University of Maryland School of Medicine, Baltimore, MD.

al., 1971; Allen and Blinks, 1979; Blinks et al., 1982). We also use the model to consider the effects of the kinetics of the reaction between calcium and aequorin (Hastings et al., 1969) on the recorded light signals and their interpretation.

METHODS

In developing this model we used, as far as possible, published information for the various parameters involved. There were three parameters for which we found no published information; (*a*) the maximum permeability of the terminal cisternae to calcium during activation, (*b*) the resting permeability of the SR, and (*c*) the rate constant for the dissociation of calcium from calsequestrin. These parameters were therefore adjusted to obtain the optimum fit between the predictions of the model and experimental measurements of myoplasmic [Ca^{2+}].

The model was based on the half sarcomere of a skeletal myofibril (Fig. 1). This structure was chosen because it contains a full complement of contractile and activating proteins (Huxley, 1971) and the myofilaments are surrounded by a network of SR (Peachey, 1965) that releases and sequesters calcium (Somlyo et al., 1981; MacLennan and Holland, 1975). Moreover, each myofibril has branches of the T-tubule system surrounding it at the level of the Z-line, so the action potential, which is conducted from the surface membrane into the T-tubule system, can synchronize the release of calcium from the terminal cisternae (Costantin, 1975).

The various components of the model are described below. Numerical values for model parameters and their sources are summarized in Table I. Many of these parameters were measured at room temperature, so we have adjusted the remaining parameters to 20°C. The experimental results presented here were also obtained at 20°C.

Geometry

The half sarcomere was assumed to be circular in cross section with a radius of 0.5 μm and a length of 1.1 μm (Peachy, 1965). Thus, the model volume was 0.86 μm^3 (0.86×10^{-15} liters). One end of the half sarcomere was at the Z-line, the region where T-tubule and SR apposition occurs; the other end was at the M-line, which lies in the middle of the sarcomere (see Fig. 1). The half sarcomere was split into four separate regions. Fig. 1 summarizes the geometry of the model and indicates the binding sites within each region and the movements of calcium between the regions. We have assumed that the longitudinal SR is continuous around the myofibril, whereas in reality, although the terminal cisternae are continuous, the longitudinal SR is discontinuous (Peachy, 1965). This simplification allows the model to have circumferential symmetry.

The volumes of the various compartments are taken from Mobley and Eisenberg (1965). (*a*) The myofibrillar space constituted 85% of the total volume. Within this region calcium was free to diffuse and to react with T- and P-sites. (*b*) The extramyofibrillar space constituted 6% of the model volume and contained P-sites only. This region lay between the SR and the myofibrillar space. Calcium was free to diffuse in this region and into the myofibrillar space, but exchange with the SR was restricted to the leak, the time-dependent permeability increase, and the calcium pump

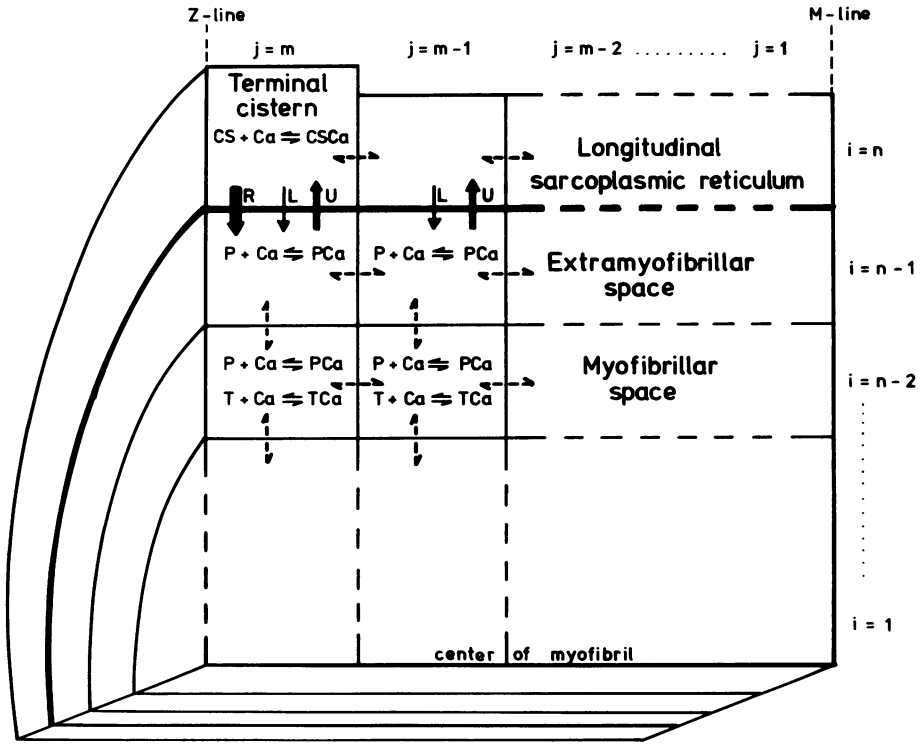

FIGURE 1 Diagram showing the geometry, calcium movements, and calcium binding sites in the model. The complete model is cylindrical and has cylindrical symmetry; this diagram depicts the elements in a representative segment from the cylinder. The outermost shell of elements ($i = n$) represents the SR. The element of this shell nearest the Z-line ($j = m$) represents the terminal cistern and contains calsequestrin (*CS*). Calcium is free to diffuse along the SR (dashed arrows between elements). The next shell of elements ($i = n - 1$) represents the extramyofibrillar space and contains P-sites (parvalbumin and high-affinity troponin sites). Calcium is free to diffuse along this shell and into the myofibrillar space (dashed arrows). Calcium movements between the SR and the extramyofibrillar space are confined to calcium release (*R*) from the terminal cisternae, a small constant calcium leak (*L*) from each SR element and calcium uptake (*U*) from the extramyofibrillar space by the SR calcium pump. The remaining inner shells ($i = n - 2, n - 3, \ldots 1$) represent the myofibrillar space. Each element contains both T-sites (low-affinity troponin sites) and P-sites. Calcium is free to diffuse between each element and its four neighbors (dashed arrows).

TABLE I
NUMERICAL VALUES AND THE SOURCE OF PARAMETERS USED IN THE MODEL

Calcium movements		
Free diffusion coefficient	7×10^{-4} mm^2 s^{-1}	(Wang, 1953)
Calcium release from terminal cisternae	Peak permeability 0.062 mm s^{-1}	(present study)
	Time course γ_{on} 1 ms γ_{off} 5 ms	(Kovacs et al., 1979)
Calcium leak from SR	Permeability 0.014×10^{-3} mm s^{-1}	(present study)
Calcium uptake by SR pump	Maximum rate 1 mM s^{-1} l^{-1}	(Ogawa et al., 1981)
	Half maximal rate (K_m) 1 μM	(Ogawa et al., 1981)
Geometry		
Half sarcomere dimension	Radius 0.5 μm, length 1.1 μm	(Peachy, 1965)
Percent volume of compartments	Myofilament space 85%	(Mobley and Eisenberg, 1965)
	Extramyofilament space 6%	
	Terminal cisternae 3.5%	
	Longitudinal SR 5.5%	
Calcium-binding proteins		
T-sites	Local concentration 140 μM	(Ebashi et al., 1969)
	Ca binding constant 10^6 M^{-1}	(Robertson et al., 1981; Zot and Potter, 1982)
	Ca on rate 1.2×10^8 M^{-1} s^{-1}	(Robertson et al., 1981)
P-sites	Local concentration 940 μM	(Gosselyn-Rey and Gerday, 1977)
	Ca binding constant 2.5×10^8 M^{-1}	(Robertson et al., 1981)
	Ca on rate 2.5×10^8 M^{-1} s^{-1}	(Robertson et al., 1981)
	Mg binding constant 1.1×10^4 M^{-1}	(Robertson et al., 1981)
	Mg on rate 6.6×10^4 M^{-1} s^{-1}	(Robertson et al., 1981)
Calsequestrin	Local concentration 31 mM	(MacLennan and Wong, 1971)
	Ca binding constant 1.2×10^3 mM^{-1}	(Ostwald and MacLennan, 1974)
	Ca on rate 240 M^{-1} s^{-1}	(present study)
Free metal concentrations		
Resting myoplasmic [Ca^{2+}]	0.06 μM	(Coray et al., 1980; Snowdowne, 1979)
Peak myoplasmic (twitch) [Ca^{2+}]	7 μM	(Blinks et al., 1978; Miledi et al., 1982)
Resting SR [Ca^{2+}]	1.5 mM	(Somlyo et al., 1981; Hasselbach, 1979)
Myoplasmic [Mg^{2+}]	3.3 mM	(Hess et al., 1982)

described below. (*c*) The longitudinal SR represented 5.5% of the model volume. It contained no calcium binding sites, and calcium was free to diffuse longitudinally. Thus, when calcium was released from the terminal cisternae during activation, calcium diffused down the longitudinal SR to the terminal cisternae. The calcium pump, whose properties are described above, lay in its walls as did the leak permeability to calcium. (*d*) The terminal cisternae constituted 3.5% of the model volume. This region contained calsequestrin, and diffusion within it was assumed to be instantaneous. Calcium was free to diffuse into it from the longitudinal SR. Its walls contained both the calcium pump and the leak permeability with the same properties as the longitudinal SR, but represented the only region with the time-dependent increase in calcium permeability that produced activation.

Calcium Movements

Calcium was assumed to diffuse along the SR and throughout the extramyofibrillar and myofibrillar spaces (dashed arrows in Fig. 1). The free diffusion coefficient of calcium in water was taken as 7×10^{-4} mm^2 s^{-1} (Wang, 1953). The apparent rate of diffusion of calcium in the myoplasm was, however, very much slower than the free-diffusion coefficient suggests because the binding of calcium to the various calcium-binding proteins slows the movement of calcium by diffusion (Kushmeric and Podolsky, 1969; Crank, 1975). Diffusion of calcium bound to soluble calcium binding proteins, e.g., parvalbumin, was ignored.

Movement of calcium from the SR to the extramyofibrillar space was assumed to occur by two processes. A constant leak between the SR and the extramyofibrillar space was incorporated, so the resting myoplasmic [Ca^{2+}] of the model was similar to that measured in resting skeletal muscle. During activation, a much larger but transient permeability change occurred, but the time course and magnitude of the permeability change involved have not been directly measured. The calcium release process has been assumed to occur without any significant change in potential across the SR. For a discussion of the experimental evidence on this point, see Oetliker, 1982. We have assumed the permeability (P_t) to turn on and off exponentially with time constants (τ_{on} = 1 ms; τ_{off} = 5 ms) that are similar (after adjustment for temperature) to those of the charge movements that are thought to be associated with activation (Schneider and Chandler, 1973; Kovacs et al., 1979). Thus

$$P_t = P_{max}[1 - \exp(-t/\tau_{on})][\exp(-t/\tau_{off})]. \quad (1)$$

The maximum permeability (P_{max}) was adjusted so that the peak myoplasmic [Ca^{2+}] in a twitch was similar to published experimental results. The free calcium concentration in the SR (SR [Ca^{2+}]) was assumed to be 1.5 mM at rest. This value lies between the estimate of 0.5–1.0 mM by Somlyo et al. (1982) and the estimate of 2.0–5.0 mM by Hasselbach (1969).

The return of calcium from extramyofibrillar space to SR was assumed, for simplicity, to result from a saturatable first-order pump, although the actual kinetics of the pump are undoubtedly more complex than this (MacLennan and Holland, 1975). The maximum pump rate (V_{max}) was 1 mM s^{-1} liter^{-1} of fiber volume, and the concentration of which half-maximal pump rate occurred (K_m) was 1 μM (Ogawa et al., 1981). Thus, the uptake of calcium into the SR as a consequence of pump activity was

$$\frac{dCa}{dt} = \frac{V_{max}[Ca^{2+}]_{ems}}{[Ca^{2+}]_{ems} + K_m} \quad (2)$$

where $[Ca^{2+}]_{ems}$ is the free calcium concentration in the adjacent element of the extramyofibrillar space.

Calcium Binding Sites

The concentration of troponin in muscle is ~70 μM (Ebashi et al., 1969), and we assumed it was uniformly distributed throughout the myofibrillar space and that it provided 140-μM low-affinity calcium binding sites (T-sites). The reaction between T-sites and calcium was modeled with an on rate constant of 1.2×10^8 M^{-1} s^{-1} and an off rate constant of 120 s^{-1} (binding constant 10^6 M^{-1}). This value represents a compromise between the values used by Robertson et al. (1981) and Gillis et al. (1982) (binding constants 3–5 $\times$ 10^6) and the more recent value (5×10^5) found in intact thin filaments (Potter and Zot, 1982). The high-affinity sites of troponin, which have similar binding kinetics to parvalbumin (Robertson et al., 1981), were, for simplicity, considered to have the same properties and distribution as parvalbumin.

The concentration of parvalbumin was taken as 400 μM (Gosselyn-Rey and Gerday, 1977) and it was assumed to be uniformly distributed through the myofibrillar and extramyofibrillar space. Because parvalbumin has two high-affinity calcium binding sites, with the inclusion of the high-affinity troponin sites, this leads to 940-μM high-affinity or P-sites. The on rate constant for calcium was taken as 2.5×10^8 M^{-1} s^{-1} and the off rate constant as 1 s^{-1} (Robertson et al., 1981). Magnesium competes with calcium for binding to the P-site and the Mg on rate constant was 6.6×10^4 M^{-1} s^{-1} and the off rate constant 6 s^{-1} (Robertson et al., 1981). The myoplasmic $[Mg^{2+}]$ was assumed to remain constant at 3.3 mM (Hess et al., 1982).

The calsequestrin content of muscle was assumed to provide 1.2 mmol calcium binding sites per liter muscle (MacLennan and Wong, 1971). It was located entirely in the terminal cisternae of the SR (Jorgensen et al., 1979) leading to 31 mM of calcium binding sites in this region. The binding constant for calcium was taken as 1.2×10^3 M^{-1} (Ostwald and MacLennan, 1974, but the on and off rate constants do not appear to have been measured.

Calcium was assumed to bind to each of the above sites without cooperativity between the sites. Thus for any site S

$$\mathrm{Ca} + S \underset{k_{off}}{\overset{k_{on}}{\rightleftharpoons}} S\mathrm{Ca}$$

so that the net flux of calcium associated with binding to the site S is

$$\frac{d[S\mathrm{Ca}]}{dt} = k_{on}[\mathrm{Ca}][S] - k_{off}[S\mathrm{Ca}]. \quad (3)$$

For the P-site, magnesium competed with calcium for the binding site and an equivalent additional set of equations was used.

Computing Methods

In this model, movements of calcium through the compartments depended on both diffusion and the binding of calcium to various sites. The general equation that describes the rate-of-change-of-reactant concentration at a point is

$$\frac{\partial C}{\partial t} = D\nabla^2 C - F(C,t) \quad (4)$$

(Crank, 1975, p. 329) where $D\nabla^2 C$ is the diffusion term and $F(C,t)$ is the net binding flux of the form given in Eq. 3 (D = free diffusion coefficient, ∇^2 is the Laplacian operator, C = free concentration of reactant). When applied to a cylinder with circumferential symmetry, the equation becomes

$$\frac{\partial C}{\partial t} = \frac{1}{r} \cdot \frac{\partial}{\partial r}\left[D \cdot r \cdot \frac{\partial C}{\partial r}\right] + \frac{\partial}{\partial x}\left[D \cdot \frac{\partial C}{\partial x}\right] - F(C,t) \quad (5)$$

where r is the radial coordinate and x is the longitudinal coordinate of the cylinder. To obtain a numerical solution for this equation, the half sarcomere was divided into n elements radially and m elements longitudinally. The volume of myofibrillar elements was set equal by making the radial elements linear with the square of the distance from the axis. Each element was addressed by subscripts i,j (see Fig. 1) where i represented the radial address (i = 1, 2, ... n; 1 at the centre of the myofibril) and j represented the longitudinal address (j = 1, 2, ... m; 1 nearest the Z line). Using this nomenclature and the finite-difference method for approximating the partial derivatives associated with diffusion (Crank, 1975; Chapt. 8), Eq. 5 for the element i,j becomes

$$\frac{\partial C_{i,j}}{\partial t} = 4Dn/B^2\,[i(C_{i+1,j} - C_{i,j}) - (i-1)(C_{i,j} - C_{i-1,j})] + D(m/L)^2\,[C_{i,j+1} - 2 \cdot C_{i,j} + C_{i,j-1}] - F(C_{i,j},t). \quad (6)$$

This equation was integrated numerically with respect to time in each element to obtain the actual concentration of calcium in each element as a function of time.

The equation for elements of the SR also contained the constant leak term and the pump term (Eq. 2) but lacked the radial diffusion term. The terminal cisternal element contained an additional term representing the time-dependent calcium permeability. The rate of calcium release was

$$\frac{d[\mathrm{Ca}]}{dt} = P_t A([\mathrm{Ca}^{2+}]_{tc} - [\mathrm{Ca}^{2+}]_x) \quad (7)$$

where P_t is the time-dependent permeability factor (Eq. 1), A is the surface area of the terminal cisternae, $[\mathrm{Ca}^{2+}]_{tc}$ is the free-calcium concentration in the terminal cisternae and $[\mathrm{Ca}^{2+}]_x$ is the free-calcium concentration in the nearest element of the extramyofibrillar space to the terminal cisternae ($i = n - 1$, $j = m$). The two outer radial elements $i = n$ and $i = n - 1$, represented the SR and the extramyofibrillar space, respectively. The element of the SR nearest the Z-line, $j = m$, represented the terminal cisternae of the SR. These compartments had different volumes from the other elements in the model; allowance was made for this when the $[\mathrm{Ca}^{2+}]$ that resulted from a given flux was calculated.

Considerations of symmetry led to the conclusion that there was no calcium flux across any of the external boundaries of the model, and this boundary condition was assumed in the model.

The model was programmed in the language Facsimile (Chance et al., 1977), which has been designed for the numerical solution of stiff differential equations and uses the method of integration described by Gear (1971). Limitations of the available computer placed an upper limit on the number of elements in the model: for the full model the half sarcomere was divided into 12 radial and 10 longitudinal elements. Comparisons with an analytical solution for radial and longitudinal diffusion in a uniform cylinder (Crank, 1975) (with suitable reductions in the model complexity) indicated errors of <4% of the true value in the computation of both longitudinal and radial diffusion gradients. The simplified model was also run with T-sites present, but in increased concentration and with faster kinetics so that the model could be compared with the analytical solution for diffusion in the presence of instantaneous, linear binding (Crank, 1975). The largest errors were again <4%. These errors resulted from the finite difference method used for evaluating the partial derivatives.

The total amount of calcium remained constant throughout the cycle of activation in this model. The program calculated this total at each instant throughout the simulation, and it remained constant to better than 1 in 10^5. This indicated that mass conservation was achieved and that truncation errors were negligible.

Aequorin light signals were simulated by assuming that aequorin was evenly distributed throughout the myofibrillar space and extramyofibrillar space. Aequorin gives a signal that is proportional to $[\mathrm{Ca}^{2+}]^{2.5}$ in the steady state, provided the calcium is spatially uniform (Allen et al., 1977). For transient changes in $[\mathrm{Ca}^{2+}]$ the aequorin reaction acts like a first-order filter causing the aequorin light signal (L) to lag behind $[\mathrm{Ca}^{2+}]^{2.5}$ with a time constant (τ) of 9 ms at 20°C (Hastings et al., 1969;

Neering and Wier, 1980). This relation was described by the following equation in which k is a proportionality constant:

$$L = k[Ca^{2+}]^{2.5} - \frac{\tau dL}{dt}. \quad (8)$$

Aequorin Experiments

Single fibers were dissected from the tibialis anterior muscle of the frog (*Rana temporaria*). Injection of aequorin and recording of light signals were similar to the methods described by Blinks et al. (1978). The light signals were filtered with a low-pass filter, time constant 0.5 ms, which reduced the noise associated with the random arrival of photons but did not significantly distort the light signal on the time scale of interest in these experiments.

RESULTS

Comparison of Experiments and Model Light Responses

Fig. 2 demonstrates that the model generates myoplasmic $[Ca^{2+}]$ during twitches and tetani that are similar to those measured experimentally. Fig. 2 *A* shows the experimentally recorded light and tension from an aequorin-injected single fiber during both a twitch and a tetanus (note the different time scales). Fig. 2 *B* shows the light output of the model and demonstrates that the model has all the major features of the experimental results. During a twitch, the model light rose to a peak at 7 ms compared with 10–15 ms for the experimentally observed light. The model light then fell, becoming approximately exponential with a half time of ~7 ms. The experimentally observed half time over the same period was 7–9 ms. During the tetanus, the model reproduced the initial fall in peak light associated with each stimulus and the subsequent rise.

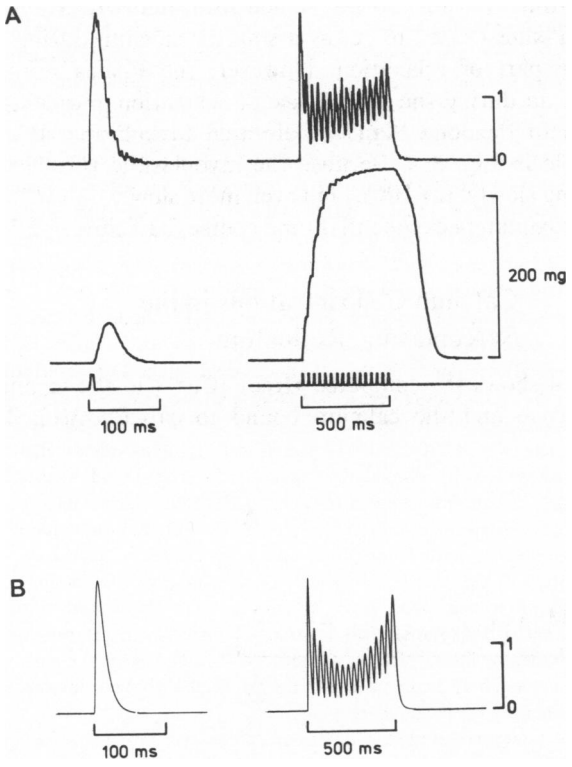

FIGURE 2 Comparison of experimental aequorin light responses with light responses from the model. *A* (*top* trace), light recorded from an aequorin-injected frog skeletal muscle fiber and (*middle* trace) the tension produced. The *lowest* trace shows the stimulus pattern. On the *left* a single stimulus gave a twitch, on the *right* a series of stimuli (30 Hz for 0.5 s) gave a just-fused tetanus. *B*, shows the light response produced by the model under identical stimulating conditions. The scale of the light records in *A* and *B* is shown by a bar on which *1* represents the light generated in the steady state by a myoplasmic $[Ca^{2+}]$ of 5 μM. Note different time scales used for the twitch and tetanus.

Calcium Concentration in the Myoplasm of the Model

The resting myoplasmic $[Ca^{2+}]$ of the model was 0.06 μM, similar to that measured experimentally in resting skeletal muscle (Snowdowne, 1979; Coray et al., 1980). In the model, the resting $[Ca^{2+}]$ was achieved by a continuous leak from the SR that balanced the SR pump uptake at the resting $[Ca^{2+}]$. The required leak flux was 57 μmol/liter/s, which represents an SR permeability of 0.014×10^{-3} mm/s assuming an SR surface area of 2×10^9 mm^2/liter (Mobley and Eisenberg, 1965).

Fig. 3 *A* shows the myoplasmic $[Ca^{2+}]$ averaged across the myofibrillar and extramyofibrillar space during a twitch and a tetanus. As noted in the methods, the peak permeability of the terminal cisternae was adjusted until the peak myoplasmic $[Ca^{2+}]$ in a twitch (7 μM) was similar to that reported experimentally (Blinks et al., 1978;

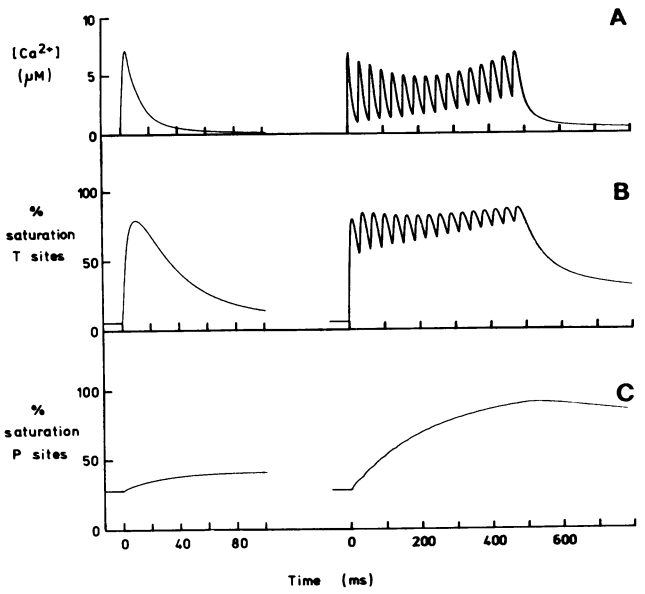

FIGURE 3 The free and bound calcium in the myoplasm generated by the model. Each panel shows a twitch on the *left* and a tetanus on the *right* on different time scales. *A*, the free calcium concentration averaged across the myoplasm. *B*, the percentage saturation of T-sites (low-affinity troponin sites) by calcium, averaged across the myoplasm. *C*, the percentage saturation of P-sites (parvalbumin and high-affinity troponin sites) with calcium, averaged across the myoplasm.

Allen and Blinks, 1979; Miledi et al., 1982). The required peak flux (37 μmol/liter/ms) occurred at a time when the terminal cistern [Ca^{2+}] was 1.1 mM and the neighboring extramyofibrillar element had a [Ca^{2+}] of 27 μM. Taking the terminal cistern membrane area as 0.54×10^9 mm^2/liter muscle (Mobley and Eisenberg, 1965), this leds to a peak permeability of 0.062 mm/s.

The rate of rise of myoplasmic [Ca^{2+}] in the model was largely determined by the 1-ms time constant given to the rise of SR permeability. The permeability function peaks at 1.7 ms and the peak flux occurred even earlier because of the rapid depletion of terminal cistern (free) [Ca^{2+}]. If there was no uptake of calcium in the model, the myoplasmic [Ca^{2+}] would simply be the integral of influx and would not show a peak. In the model, the peak myoplasmic [Ca^{2+}] occurred at 3 ms when uptake by the SR and the P and T-sites became greater than the residual influx from the terminal cisternae. The aequorin light signal lagged behind the [Ca^{2+}] changes and this resulted in a peak light signal at 7 ms. The rate of fall of myoplasmic [Ca^{2+}] in a twitch in the model was determined by two factors; (*a*) the rate of extrusion of calcium from the myoplasm by the SR calcium pump and (*b*) the uptake of calcium by the P-sites, which continued during relaxation (Fig. 3 *C*).

Figs. 3 *B* and 3 *C* show the concentration of calcium bound to the T-sites of troponin ([TCa]) and the P-sites ([PCa]). The saturation of the T-sites with calcium was 6% at rest and rose to 79% at the peak of a twitch and 86% at the end of the tetanus, but clearly these numbers depended on the binding constant choosen for the T-sites, about which uncertainty exists (see Methods).

The peak of calcium binding to T-sites ([TCa]) occurred at ~10 ms. The delay between peak myoplasmic [Ca^{2+}] (3 ms) and peak [TCa] (10 ms) was due in part to the kinetics of calcium binding to T-sites, but a significant additional delay resulted from diffusion. Delays due to binding kinetics alone could be assessed by examination of the [Ca^{2+}] and [TCa] in a single element of the model. Thus, in the myofibrillar element that lay closest to the terminal cistern, peak [Ca^{2+}] occurred at 1–2 ms, whereas peak [TCa] occurred at 3–4 ms. The rather longer delays seen in the spatially averaged results (Fig. 3) can be attributed to the effects of diffusion across the myofibril. On the other hand, during the falling phase of [Ca^{2+}] there was a substantial lag between myoplasmic [Ca^{2+}] and the fall of [TCa], reflecting the much slower rate of dissociation of calcium from T-sites.

The P-sites had a higher affinity for calcium than the T-sites, and also a significant affinity for magnesium. Consequently, at rest the P-sites were 98% saturated with 28% as PCa and 70% PMg. During a twitch or a tetanus, [PCa] increases because of the elevated myoplasmic [Ca^{2+}], but at a rate that is dominated by the relatively slow rate at which magnesium dissociates from P-sites. Because the P-sites equilibrated slowly and because myoplasmic [Ca^{2+}] was still elevated during relaxation, P-sites continued to bind calcium during relaxation until ~150 ms, and therefore they contributed to the rate of fall of myoplasmic [Ca^{2+}]. In a tetanus the P-sites approached equilibrium with the elevated myoplasmic [Ca^{2+}] with a half-time of 160–180 ms. When saturated with calcium, the P-sites ceased to act as a sink for calcium during the early part of relaxation. However, the P-sites released calcium during the later phase of relaxation and contributed to the long "tail" of elevated myoplasmic [Ca^{2+}] visible in Fig. 3 *A*. Because the myoplasmic [Ca^{2+}] was falling slowly, the [PCa] fell even more slowly, but with an approximately exponential time course, half time = 2.5 s.

Calcium Concentrations in the Sarcoplasmic Reticulum

Fig. 4 shows the computed (free) [Ca^{2+}] in the terminal cisternae and the calcium bound to calsequestrin. The

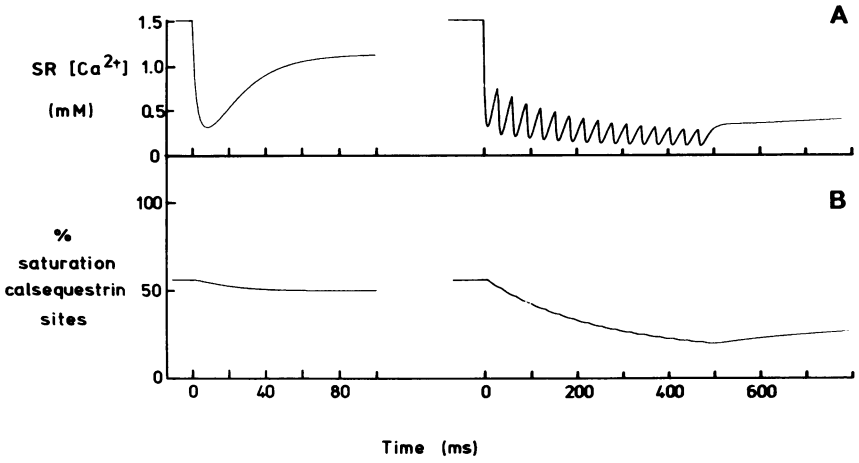

FIGURE 4 The free and bound calcium in the SR generated by the model. Same general format as Fig. 3. *A*, the free calcium concentration in the SR. *B*, the percentage saturation of calsequestrin with calcium.

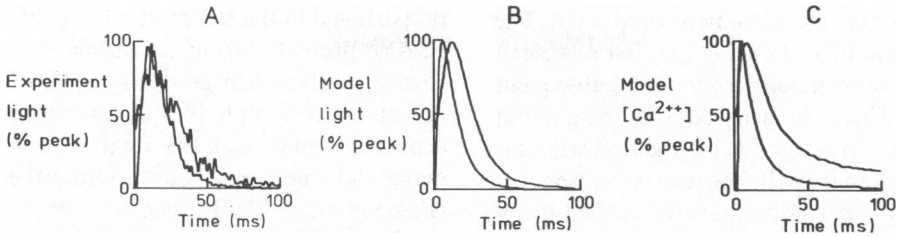

FIGURE 5 The time course of decline of myoplasmic $[Ca^{2+}]$ after a twitch and a tetanus: comparison of experimental results with model output. In each panel the stimulus of a twitch and the last stimulus of a tetanus occur at zero time. The more slowly declining record in each panel is the tetanus. *A*, the experimental light output from a twitch and a tetanus (30 Hz, 0.5 s). The peak of the twitch and the tetanus have both been adjusted to 100%. Each record is the average of four responses; the noise on the records is caused by the random arrival of photons. *B*, model light output averaged across the myoplasm and displayed on the same format as *A*. *C*, model myoplasmic $[Ca^{2+}]$ displayed on the same format as *A*.

$[Ca^{2+}]$ fell rapidly during a twitch and then recovered more slowly, principally due to release of calcium bound to calsequestrin. As noted in Methods, although the binding constant of calsequestrin has been measured, the apparent on and off rates for calcium binding do not appear to have been measured. We chose an apparent off rate constant ($5\ s^{-1}$), which gives a slow fall of calcium bound to calsequestrin during a tetanus and leads to an appropriately shaped myoplasmic $[Ca^{2+}]$ during a tetanus.

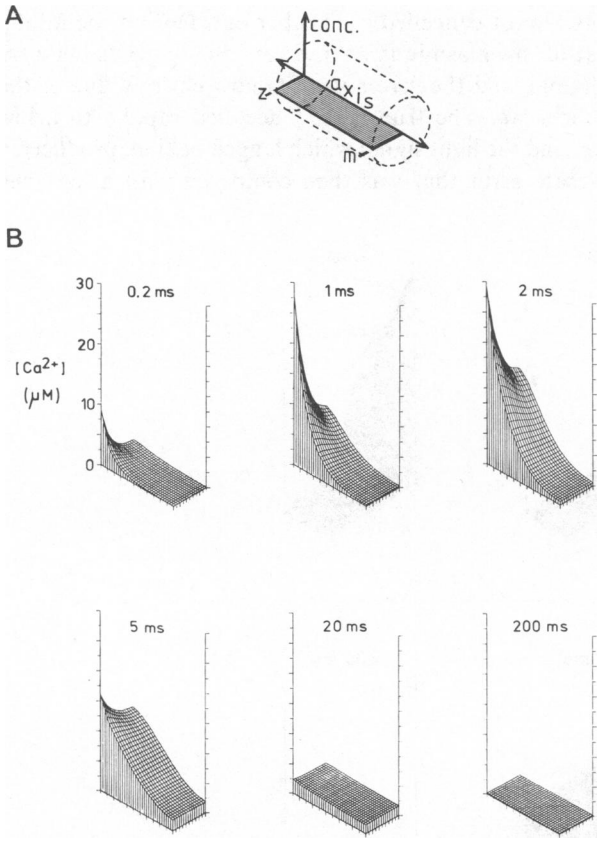

FIGURE 6 $[Ca^{2+}]$ across the myofibrillar space during a twitch. *A* depicts the general format of the display used in *B* and Fig. 7. Vertical distances represent concentration (conc.). The base represents a section through the sarcomere oriented as shown in *A*. Each plot in *B* shows the concentrations of free calcium across the sarcomere at the time indicated.

The integrated calcium flux across the terminal cisternae membrane in response to the first stimulus of a tetanus was 153 μmol/liter in the second 92, the third 81, and by the end of the tetanus it was still falling, though very slowly, and amounted to 37 μmol/liter. Fig. 4 *B* shows that the recovery of $[Ca^{2+}]$ in the terminal cisternae had a fast and a subsequent slow phase. The fast phase was due to rapid uptake of calcium by the SR pump and the redistribution of calcium along the SR by diffusion; diffusion was relatively rapid along the longitudinal SR because the absence of calcium binding sites. The slow phase represented the gradual release of calcium from P-sites in the myoplasm, and had a similar half time (2.5 s) to that found for the fall of [PCa].

The Rate of Decline of $[Ca^{2+}]$ After Twitches and Tetani

Both Blinks et al. (1978) and Miledi et al. (1982) showed that the rate of fall of $[Ca^{2+}]$ was faster after a twitch than after a tetanus. This point is demonstrated in Fig. 5 *A*, which shows the light signal from a twitch superimposed on the light signal that followed the last stimulus of a 0.5 s tetanus (note that the records have been normalized to have the same maxima). The record from the tetanus started at 40% of maximum, reached its peak later, declined more slowly, and showed a prolonged elevated "tail" of light. Fig. 5 *B* shows that the model light reproduced all of these features. Fig. 5 *C* shows the model myoplasmic $[Ca^{2+}]$; comparison of *B* and *C* illustrates the distorting effects of the aequorin kinetics and nonlinearity.

Gradients of Calcium in the Myoplasm

In this model, calcium is released solely from the terminal cisternae; this leads to a substantial but transient gradients of myoplasmic $[Ca^{2+}]$ both radially and longitudinally (Fig. 6). These gradients were largest at the peak of the permeability function (~2 ms) and immediately adjacent to the release sites at the terminal cisternae. However, the gradients in myoplasmic $[Ca^{2+}]$ declined rapidly when release had terminated, so that by 20 ms and throughout

relaxation, gradients across the sarcomere were small. The gradients in myoplasmic [Ca^{2+}] during the first release of calcium of a tetanus were much larger than subsequent releases (not shown). This was partly because the amount of calcium released was largest following the first stimulus of a tetanus (Fig. 4 *A*) and partly because on subsequent releases, the T-sites were partially saturated at the time of release so that the apparent rate of diffusion of calcium was faster and diffusion gradients were more short-lived.

The gradients of [TCa] (Fig. 7) differed in two respects from those of [Ca^{2+}]. First, because the relation between [TCa] and [Ca^{2+}] saturated as [Ca^{2+}] rose above 5–10 μM, the gradients of [TCa] became small when the [Ca^{2+}] was above this level. This effect was clear at 5 ms when close to the Z-line, the T sites of troponin were 90% saturated and gradients of [TCa] were small despite large gradients of [Ca^{2+}]. Second, because the dissociation of Ca from the T site of troponin was relatively slow, the gradients of [TCa] persisted much longer than those of [Ca^{2+}] and were still substantial at 10–20 ms.

Errors in the Estimation of Myoplasmic [Ca^{2+}] Using Aequorin

When gradients of myoplasmic [Ca^{2+}] are present, the signal from a [Ca^{2+}] indicator will depend on its location in the cell with respect to the gradients. Even if the [Ca^{2+}] indicator is uniformly distributed across the regions where the gradients exist, the indicator signal will be hard to interpret if the relation between the indicator signal and [Ca^{2+}] is nonlinear. For aequorin, the light signal is proportional in the steady state to [Ca^{2+}]$^{2.5}$ in the range of [Ca^{2+}] present during activation (Allen et al., 1977). Consequently, when gradients of [Ca^{2+}] are present, the regions with a high [Ca^{2+}] tend to dominate the total aequorin signal, and the total aequorin signal overestimates the true mean [Ca^{2+}] across the region of interest (Baker et al., 1971; Blinks et al., 1982).

Our model allowed us to estimate the size of this error, and this has been done in Fig. 8. *A* shows the mean myoplasmic [Ca^{2+}] across the sarcomere that the model generates. The light signal was then calculated (Eq. 8) for each element of the sarcomere (thus introducing the lag due to aequorin kinetics). The mean light signal from all the elements obtained in this way was then raised to the power of 1/2.5 to yield an estimated myoplasmic [Ca^{2+}] (Fig. 8 *B*). This estimated myoplasmic [Ca^{2+}] would be in error whenever myoplasmic [Ca^{2+}] was changing, because the light signal lagged behind the myoplasmic [Ca^{2+}], and whenever there were gradients of myoplasmic [Ca^{2+}] present. Fig. 8 *C* shows the size of these errors expressed as a percentage of the true myoplasmic [Ca^{2+}]. The error was small during the rising phase of the myoplasmic [Ca^{2+}] of a twitch, because errors due to gradients tended to increase the estimated myoplasmic [Ca^{2+}], whereas the error due to the aequorin lag was in the opposite direction, and the two errors almost cancelled each other out. During the falling phase of myoplasmic [Ca^{2+}], errors due to gradients were negligible, and the errors were almost entirely due to the aequorin lag. The true [Ca^{2+}] declined rapidly to a low value, and the light signal which lagged behind, produced a moderate error that was then compared with a low true

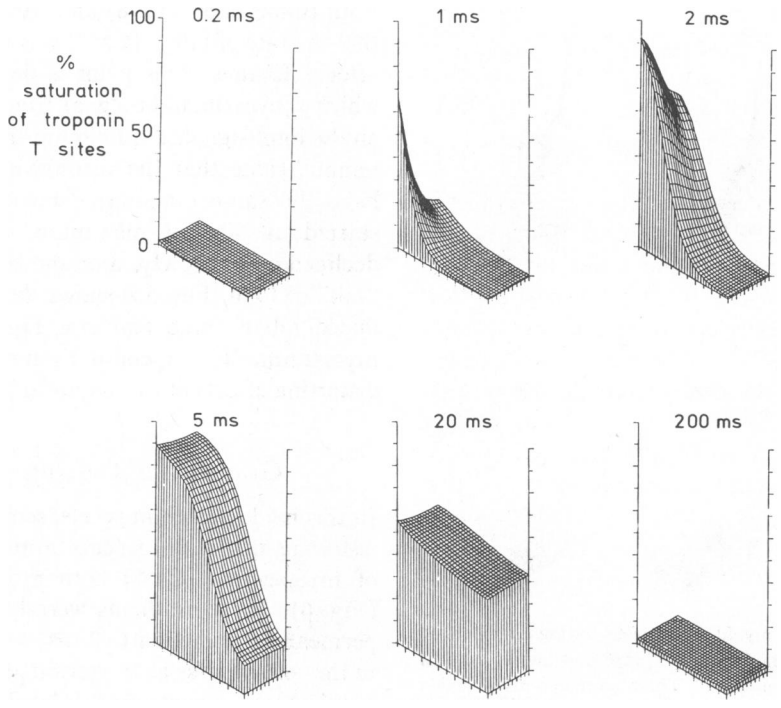

FIGURE 7 Occupancy of T-site with calcium across the myofibrillar space. Same format as Fig. 6.

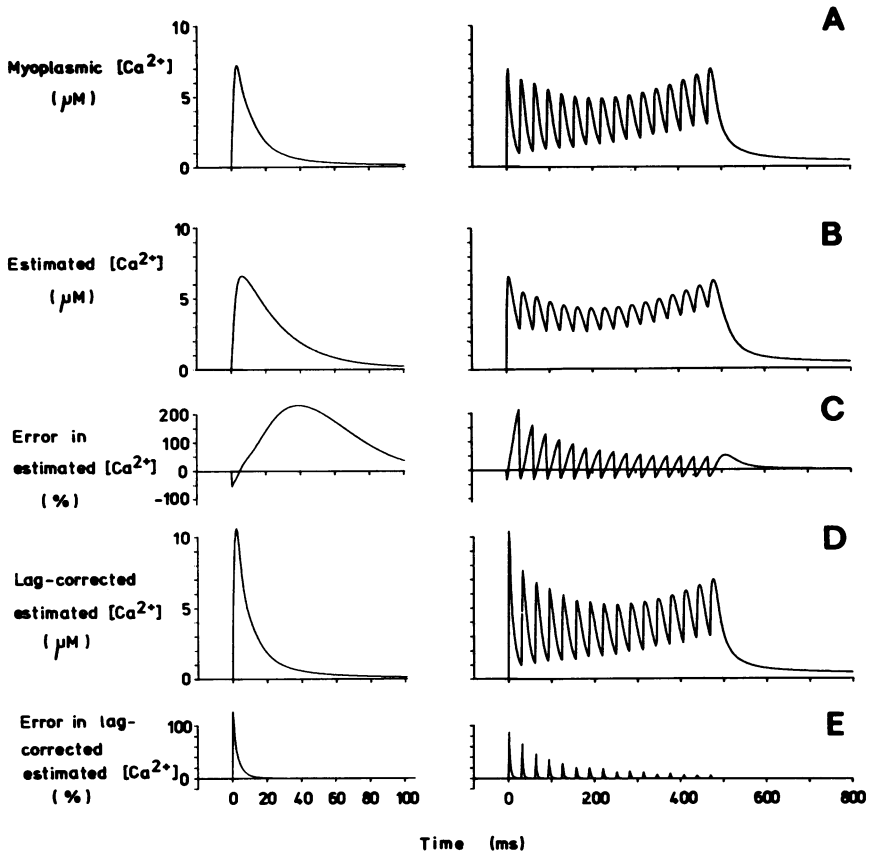

FIGURE 8 The errors in estimation of $[Ca^{2+}]$ from aequorin light signals. All panels show model outputs averaged across the myoplasm and show a twitch on the right and a tetanus on the left. *A*, mean myoplasmic $[Ca^{2+}]$ generated by the model. *B*, estimated $[Ca^{2+}]$ obtained by converting the $[Ca^{2+}]$ signal in *A* to light and then applying the calibration procedure, which does not correct for aequorin lag, to reconvert it $[Ca^{2+}]$ (see Methods and Results for further details). *C*, error in *B* calculated as 100 × (estimated $[Ca^{2+}]$ − true $[Ca^{2+}]$)/true $[Ca^{2+}]$. *D*, estimated $[Ca^{2+}]$ obtained by lag-correcting the light signal and then applying the calibration procedure to convert to $[Ca^{2+}]$. *E*, error in *D* calculated with the same formula as given above.

value leading to a large relative error. The errors decreased during a tetanus because the myoplasmic $[Ca^{2+}]$ fell more slowly after each release, leading to a smaller error due to the lag.

If the light signal was corrected for aequorin kinetics (Ashley and Moisescu, 1972; Allen and Blinks, 1979; Neering and Wier, 1980) before converting it to $[Ca^{2+}]$, then the estimated myoplasmic $[Ca^{2+}]$ shown in Fig. 8 *D* was obtained. The remaining errors were entirely due to gradients of myoplasmic $[Ca^{2+}]$. These errors were largest (120%) during the rising phase of calcium during a twitch or the first calcium release of a tetanus, but became smaller in subsequent releases, both because calcium release fell and because the increasing saturation of T-sites by calcium allowed the apparent rate of diffusion of calcium to increase.

DISCUSSION

This model had two conceptually separate parts. One part was concerned with the amount of calcium released by each action potential and the resultant changes in free and bound calcium in the SR and the myoplasm. This part of the model predicted the time course and amplitude of the myoplasmic $[Ca^{2+}]$ during twitches and tetani with reasonable accuracy. The other part of the model was concerned with the estimation of calcium gradients across the myoplasm. These results allowed us to consider how gradients of $[Ca^{2+}]$ and calcium bound to troponin T-sites ([TCa]) would affect muscle activation. In addition the model allowed us to estimate the errors associated with the conversion of aequorin light signals to myoplasmic $[Ca^{2+}]$.

Our model had some features in common with the models recently published by Robertson et al. (1981) and by Gillis et al. (1982). The model of Robertson et al. examined the changes in occupancy of T and P sites when transient increases of $[Ca^{2+}]$ of constant amplitude and time course were imposed on them. The model of Gillis et al. examined both occupancy of sites and the $[Ca^{2+}]$ that resulted when a constant amount of calcium (200 μmol/liter muscle) was released into appropriate concentrations of the T and P sites. A fall in the $[Ca^{2+}]$ was achieved by inclusion of an SR pump. Thus, in these two models, the

changes in myoplasmic $[Ca^{2+}]$, which drive the changes in calcium binding, are only crude approximations to those that are experimentally observed. In our model, the primary effect of a stimulus was to produce a transient increase in the permeability of the terminal cistern membrane. Consequently, the amount of calcium released into the myoplasm and the resulting change in myoplasmic $[Ca^{2+}]$ were functions of the free and bound calcium in both the SR and the myoplasm. Although our modeling of the release and uptake processes were undoubtedly simplifications, we know that the myoplasmic $[Ca^{2+}]$ generated by the model was very similar to that observed experimentally. Consequently the changes in saturation of the calcium binding sites estimated in our model were probably more realistic than those in the other models cited.

Myoplasmic $[Ca^{2+}]$ Generated by the Model

In this model, the resting $[Ca^{2+}]_i$ and the peak $[Ca^{2+}]_i$ in a twitch were made similar to experimentally measured values by choosing appropriate resting and peak fluxes of calcium from the SR. This approach leds to a resting SR calcium permeability of 0.014×10^{-3} mm s^{-1}. In studies of isolated SR, the calcium permeability is very low, but there is a substantial permeability to K^+, Na^+, and H^+ on the order of 0.01×10^{-3} mm s^{-1} (see Oetliker, 1982, for review). Thus our model seemed to require an unexpectedly high resting calcium permeability, compared with studies of isolated SR. This could be because the SR in vivo has an additional calcium permeability switched on even at rest. Alternatively, since in our model the resting calcium flux from the SR was chosen to balance the pump uptake at the resting $[Ca^{2+}]_i$, it may be that our model of the calcium pump was unrealistic and that pump uptake at the resting $[Ca^{2+}]_i$ is smaller than we have assumed.

The peak calcium permeability of the SR calculated in our model may be compared with the calcium fluxes associated with calcium channels. The open-channel conductance of single calcium channels are reasonably similar in a variety of tissues and are ~5 pS (Reuter, 1983). Assuming that the SR has no potential across it either at rest or during release (for discussion of this assumption see Somlyo et al., 1981; Oetliker, 1982), then the only driving force for calcium is its concentration gradient. At the time of peak calcium permeability, the SR $[Ca^{2+}]$ was 1.1 mM and the extramyofibrillar space $[Ca^{2+}]$ was 27 μM, so that the driving force was $(58/2)\log_{10}(1.1/0.027) = 47$ mV. Therefore, a peak current of 0.25 pA or 7×10^5 Ca^{2+} ions/s or 1.2×10^{-18} mol/s flowed through each calcium channel. Consequently, the peak flux in our model (36 μmol/ms/liter muscle) would require 3×10^{16} channels/liter muscle, or 30 channels/μm^3. The T-tubules and SR are connected by "feet" (Franzini-Armstrong, 1975) that have a density of 800/μm^2 of T-tubule membrane. Taking 0.22 μm^2 as the area of T-tubule/μm^3 of muscle (Mobley and Eisenberg, 1965), it appears that there are 170 feet/μm^3 of muscle. Thus, if each foot controlled a single calcium channel in the SR, each channel would have to be open ~20% of the time to achieve the peak calcium flux computed in our model.

Twitches. The time-to-peak light in our model was rather shorter than the experimentally observed value. Because the model time-to-peak light was dominated by the time constant assumed for the rise of permeability of the terminal cisternae, this suggested that our assumed time constant was too fast. An additional small part of the discrepancy might have arisen because our model did not include any delay for conduction of the action potential through the T-tubule network.

The rate of fall of light in the model during a twitch agreed well with the experimentally observed rate. Endo (1976) calculated that estimates of the uptake of calcium by the isolated SR were inadequate to explain the observed rate of fall of tension. Our results show that when we used the pump characteristics described by Ogawa et al. (1981) the rate of fall of $[Ca^{2+}]$ in the model was similar to that observed experimentally. However, not all the calcium released in a twitch (153 μmol/liter) was returned to the SR immediately. Thus, 150 ms after the stimulus, [PCa] had increased by 127 μmol/liter and this calcium did not have to be removed from the myoplasm by the SR pump during this period. Thus our model shows, in agreement with the conclusion of Gillis et al. (1982) but in contrast to that of Robertson et al. (1981), that parvalbumin made a very important contribution to the fall of $[Ca^{2+}]$ in a twitch, and therefore assisted relaxation. Of course the calcium bound to parvalbumin had to be released later when the SR had lowered the $[Ca^{2+}]$ sufficiently (see next section).

Tetani. An interesting feature of the model is that it provided a simple explanation of the initial fall and subsequent rise in peak $[Ca^{2+}]$, observed experimentally during a series of closely spaced twitches or a tetanus (Fig. 2; Blinks et al., 1978; Miledi et al., 1982). In our model, the initial fall was caused by a rapid reduction in the amount of calcium released per stimulus as both free and bound calcium in the SR became depleted. The peak myoplasmic $[Ca^{2+}]$ rose towards the end of a tetanus, despite the decreasing calcium release, because (*a*) the T and P sites were getting closer to full saturation and therefore bound less of the released calcium and (*b*) the slower fall in myoplasmic $[Ca^{2+}]$ leds to successive calcium transients, each starting from a higher initial $[Ca^{2+}]$. Blinks et al. suggested that the secondary rise in $[Ca^{2+}]$ in a tetanus was due to a slowing of the SR calcium pump. Our model makes it clear that it is not necessary to invoke this additional property to explain the phenomenon.

Our model only reproduced the initial fall and subsequent rise of myoplasmic $[Ca^{2+}]$ in the tetanus if the

amount and rate of releasable calcium in the SR was balanced by the amount and rate of uptake of calcium by binding sites in the myoplasm. Thus, any of the following changes led to progressively smaller peaks of myoplasmic [Ca^{2+}] during a tetanus (the converse leading to progressively larger peaks); reduced SR resting [Ca^{2+}], reduced calsequestrin, decreased rate of calcium release by calsequestrin, increased T-site concentration, increased P-site concentration, and increased rate of uptake of calcium by P-sites.

A further feature of the model was that the rapid fall of [Ca^{2+}] following a tetanus was succeeded by a prolonged elevation of myoplasmic [Ca^{2+}], initially at ~1 μM and falling with a half time of several seconds (Fig. 3 *A*). This phenomenon has been observed experimentally using aequorin (Cannell, 1982), though the accompanying light signal was very small because of the nonlinear relation between light and [Ca^{2+}] (compare Figs. 5 *B* and 5 *C*). It is also visible in the records of Miledi et al. (1982) although they do not discuss the underlying mechanism. The explanation for this observation in our model and presumably in reality is that parvalbumin is slowly unloading its bound calcium during this period.

Distribution of Calcium in the Sarcomere

The amounts of calcium in the various compartments of our model can be compared with the ion probe measurements of calcium made by Somlyo et al. (1981). Table II below shows the total amounts of calcium (free and bound) per unit tissue volume (millimoles per liter) measured by these workers at various sites. Their tetanic figures were obtained after 1.2 s of a tetanus at 40 Hz stimulation and at 4°C.

The ion probe measurements showed larger amounts of calcium in all compartments; this may be partly because of the differences in conditions and partly because there are other binding sites for calcium that our model did not include, e.g., the high-affinity calcium-binding protein in the SR (MacLennan and Holland, 1975) and calcium bound to membranes and other intracellular proteins. However, in other respects the similarity between Somlyo et al.'s measurements and our model is good. Thus, the fractional reduction in terminal cisternae calcium during a tetanus was similar and the principle site where this released calcium appears was in the myoplasm (bound mainly to P-sites). Neither in our model nor in the measurements of Somlyo et al. is there any accumulation of calcium in the LSR during a tetanus. This is in contrast to the earlier measurements of Winegrad (1968) whose spatial resolution may have been insufficient to distinguish between calcium bound to parvalbumin in the myoplasm and calcium bound within the longitudinal SR.

TABLE II
PREDICTED AND MEASURED CALCIUM DISTRIBUTIONS

	Somlyo et al.		Model (mmol/l)	
	Resting	Tetanus	Resting	Tetanus
	mmol/ liter	*mmol/ liter*	*mmol/ liter*	*mmol/ liter*
Terminal cisternae	33	13	24	8
Longitudinal SR	—	1.5	1.5	0.2
Myoplasm	0.7	1.4	0.3	1.0
Total cell	2.0	2.0	1.2	1.2

The Rate of Decline of Myoplasmic [Ca^{2+}] in Twitches and Tetani

The model mimics the slowing of the rate of fall of the myoplasmic [Ca^{2+}] that was observed (Fig. 5; Blinks et al., 1978; Miledi et al., 1982) when tetani were compared with twitches. The reason for this effect was that parvalbumin continued to bind calcium for up to 150 ms after a twitch. In the 30 ms following the first stimulus of a tetanus, parvalbumin took up 84 μmol Ca^{2+}/liter muscle. However, in the equivalent period after the last stimulus of a tetanus, parvalbumin was nearly saturated and only took up 11 μmol Ca^{2+}/liter muscle. Blinks et al. (1978) and Miledi et al. (1982) both suggest that slowing of SR uptake may be the cause of the slower fall of [Ca^{2+}] after a tetanus. Our model showed, however, that the presence of parvalbumin at physiological concentrations can explain this result.

Gradients of Calcium

Free diffusion of calcium over distances of 1 μm in water approaches completion in <1 ms; the substantial gradients of [Ca^{2+}] that existed in this model over at least 10 ms were caused by the slowing of diffusion associated with the binding of calcium to fixed binding sites in the cell. The effect of these gradients was that the [Ca^{2+}] was much higher close to the release sites than at the M line, during the first 10 ms of the twitch, but this gradient of [Ca^{2+}] largely disappeared after 20 ms.

In terms of activation of contraction, which depends on T-site occupation, these gradients had several effects. (*a*) They slowed the overall rate of activation. Thus, close to the terminal cisternae the peak of [TCa] occurred at 3–4 ms, whereas at the M line the peak occurred at ~20 ms. The peak averaged across the myoplasm occurred at ~10 ms, and this slowing was largely due to the effects of diffusion. (*b*) The slowing of calcium movements due to diffusion also reduced the saturation of T sites achieved in a twitch. The calcium released in a twitch (153 μmol/liter muscle) would, if instantaneously distributed, have led to 95% saturation of T sites. In fact, the maximal observed saturation was 77%, and this reduction was largely because, during the time calcium was being distributed around the sarcomere, uptake of calcium by the P-sites and the SR occurred.

The Use of Aequorin as a Calcium Indicator in Muscle

Baker et al. (1971) first described how the presence of gradients of calcium could lead to an aequorin signal that was dominated by the regions with the highest $[Ca^{2+}]$. Blinks et al. (1978) pointed out that the gradients would be greatest in a twitch and decline during a tetanus. Our model suggests that in a twitch at 20°C the combination of aequorin lag and gradients means that the peak light estimates the peak mean myoplasmic calcium rather well, though during relaxation, the aequorin lag leds to a light signal that was rather larger than the true mean myoplasmic $[Ca^{2+}]$. If lag correction was applied to the light signal, the peak light signal in a twitch substantially overestimated the mean myoplasmic $[Ca^{2+}]$. However, the errors were small during the falling phase of the light record, and the errors became progressively smaller throughout a tetanus.

Stephenson et al. (1981) suggested that proteins such as aequorin might be partially excluded from the myofibrillar space by virtue of their charge and molecular size. In contrast, Fabiato (1981) suggested that aequorin is preferentially located in the myofibrillar space. From Fig. 6 it is possible to estimate the effect on the aequorin signal that would result from such nonuniform distributions.

At 2 ms (when gradients of $[Ca^{2+}]$ are largest) the mean $[Ca^{2+}]$ in the myofibrillar space was 6.5 μM whereas the mean $[Ca^{2+}]$ in the extramyofibrillar space was 8.0 μM. Even if aequorin were totally excluded from the extramyofibrillar space, this difference would have only a small effect on the overall aequorin light signal. This is because at this early time, the aequorin signal is dominated by the relatively slow kinetics of the aequorin reaction. Exclusion of aequorin from the extramyofibrillar space had only a very small effect on the overall light signal because the extramyofibrillar space was only a small fraction of the total myoplasmic volume. At later times the gradients of calcium decline and the aequorin light signal is essentially unaffected by the distribution of aequorin. It seems therefore that even major redistributions of aequorin have only minor effects on the overall light signal.

Cardiac Muscle. Although this model deals specifically with skeletal muscle, it is of interest to consider how aequorin light signals from heart muscle might be affected by calcium gradients and aequorin kinetics. The time course of aequorin signals from heart muscle is generally substantially slower than those from skeletal muscle. Allen and Kurihara (1980) found that the time-to-peak light recorded from aequorin-injected ventricular muscles was 25–100 as in experiments on various mammalian species at 30°C. In view of the faster aequorin kinetics at this temperature and the relatively slow rate of rise of the signal, the effects of aequorin kinetics can probably be ignored. The slow time course of the aequorin signal and the fact that its amplitude was smaller (Allen and Blinks, 1979) suggested that the maximum rate of influx of calcium into the myoplasm must be considerably slower in ventricular muscle than in skeletal muscle; consequently errors due to diffusion gradients should be substantially smaller.

However, this conclusion depends critically on the assumption that the only gradients of calcium of importance are those at the sarcomere level. In skeletal muscle, the fact that myofibrils across the cell (100 μm diam) activate within several milliseconds (Costantin, 1975) provides support for this assumption. However, in cardiac muscle, the inward calcium flux comes from both inward membrane currents and release from internal stores (Chapman, 1979), and we know of no evidence as to whether these processes are uniformly distributed across the cell cross section. It is clear that, at least in Purkinje fibers, the inward membrane current of calcium occurs only at the surface of the cell, since in this tissue there are no T-tubules (Sommer and Johnson, 1979). Thus, in Purkinje fibres, modeling calcium movements at the sarcomere level alone would be inappropriate; it would also be necessary to consider gradients of calcium across the cell (Fischmeister and Horackova, 1983).

We are grateful to Dr. E. M. Chance both for initial help in the use of the Facsimile language and for assistance with mathematical aspects of the modeling. We thank Drs. D. I. Attwell and R. C. Woledge for comments on an earlier version of this manuscript.

Dr. Cannell was supported by a Medical Research Council Training Fellowship. The aequorin used in this study was prepared in the laboratory of Dr. J. R. Blinks with support from National Institutes of Health grant HL12186.

Received for publication 1 August 1983 and in final form 13 December 1983.

REFERENCES

Allen, D. G., and J. R. Blinks. 1979. The interpretation of light signals from aequorin-injected skeletal and cardiac muscle cells: a new method of calibration. *In* Detection and measurement of free Ca^{2+} in cells. C. C. Ashley and A. K. Campbell, editors. Elsevier/North Holland, New York.

Allen, D. G., J. R. Blinks, and F. G. Prendergast. 1977. Aequorin luminescence: relation of light emission to calcium concentration — a calcium independent component. *Science (Wash. DC).* 195:996–998.

Allen, D. G., and S. Kurihara. 1980. Calcium transients in mammalian ventricular muscle. *Eur. Heart J.* 1a:5–15.

Ashley, C. C., and D. G. Moisescu. 1972. Model for the action of calcium in muscle. *Nature (Lond.).* 237:208–211.

Baker, P. F., A. L. Hodgkin, and E. B. Ridgway. 1971. Depolarisation and calcium entry in squid axons. *J. Physiol. (Lond.).* 218:709–755.

Blinks, J. R., R. Rüdel, and S. R. Taylor. 1978. Calcium transients in isolated amphibian skeletal muscle fibers: detection with aequorin. *J. Physiol. (Lond.).* 277:291–323.

Blinks, J. R., W. G. Wier, P. Hess, and F. G. Prendergast. 1982. Measurement of Ca concentrations in living cells. *Prog. Biophys. Mol. Biol.* 40:1–114.

Cannell, M. B. 1982. Intracellular calcium during relaxation in frog single muscle fibers. *J. Physiol. (Lond.).* 326:70–71P.

Chance, E. M., A. R. Curtis, I. P. Jones, and C. R. Kirby. 1977. FACSIMILE: a computer programme for flow and chemistry simulation, and general initial value problems. Computer Science and Systems Division, Atomic Energy Research Establishment (AERE) Harwell, Oxfordshire, Her Majesty's Stationary Office, London.

Chapman, R. A. 1979. Excitation-contraction coupling in cardiac muscle. *Prog. Biophys. Mol. Biol.* 35:1–52.

Costantin, L. L. 1975. Contractile activation in skeletal muscle. *Prog. Biophys. Mol. Biol.* 29:197–224.

Coray, A., C. H. Fry, G. Hess, J. A. S. Mc Guigan, and R. Weingart. 1980. Resting calcium in sheep cardiac tissue and frog skeletal muscle measured with ion-selective micro-electrodes. *J. Physiol. (Lond.).* 305:60P.

Crank, J. 1975. The Mathematics of Diffusion. 2nd ed. Oxford University Press, London. 137–159.

Ebashi, S., M. Endo, and I. Ohtsuki. 1969. Control of muscle contraction. *Q. Rev. Biophys.* 28:351–384.

Endo, M. 1976. Calcium release from the sarcoplasmic reticulum. *Physiol. Rev.* 57:71–108.

Fabiato, A. 1981. Myoplasmic free calcium concentration reached during the twitch of an isolated cardiac cell and during calcium-induced release of calcium from the sarcoplasmic reticulum of a skinned cardiac cell from the adult rat or rabbit ventricle. *J. Gen. Physiol.* 78:457–497.

Fischmeister, R., and M. Horackova. 1983. Variation of intracellular Ca^{2+} following Ca^{2+} current in heart. A theoretical study of ionic diffusion inside a cylindrical cell. *Biophys. J.* 41:341–348.

Franzini-Armstrong, C. 1975. Membrane particles and transmission at the triad. *Fed. Proc.* 34:1382–1389.

Gear, C. W. 1971. The automatic integration of ordinary differential equations. *Comm. A.C.M.* 14:176–179.

Gillis, J. M., D. Thomason, J. Lefevre, and R. H. Kretsinger. 1982. Parvalbumins and muscle relaxation: a computer simulation study. *J. Muscle Res. Cell Motil.* 3:377–398.

Gosselin-Rey, C., and C. Gerday. 1977. Parvalbumins from frog skeletal muscle. Isolation and characterisation. Structural modifications associated with calcium binding. *Biochim. Biophys. Acta.* 492:53–63.

Hasselbach, W. 1979. The sarcoplasmic calcium pump. A model of energy transduction in biological membranes. *In* Topics in Current Chemistry. Berlin, Heidelberg, New York: Springer-Verlag. 78:1–56.

Hastings, J. W., G. Mitchell, P. H. Mattingly, J. R. Blinks, and M. van Leeuwen. 1969. Response of aequorin bioluminescence to rapid changes in calcium concentration. *Nature (Lond.).* 222:1047–1050.

Hess, P., P. Metzger, and R. Weingart. 1982. Free magnesium in sheep, ferret and frog striated muscle at rest measured with ion selective electrodes. *J. Physiol. (Lond.).* 333:173–188.

Huxley, H. E. 1971. The structural basis of muscular contraction. *Proc. R. Soc. B.* 160:442–448.

Jorgenson, A. O., V. Kalnins, and D. H. MacLennon. 1979. Localisation of sarcoplasmic reticulum proteins in rat skeletal muscle by immunofluorescence. *J. Cell Biol.* 80:372–384.

Kovacs, L., E. Rios, and M. Schneider. 1979. Calcium transients and intramembrane charge movement in skeletal muscle fibers. *Nature (Lond.).* 279:391–396.

Kushmeric, M. J., and R. J. Podolsky. 1969. Ionic mobility in muscle cells. *Science (Wash. DC).* 166:1297–1298.

MacLennan, D. H., and P. C. Holland. 1975. Calcium transport in sarcoplasmic reticulum. *Annu. Rev. Biophys. Bioeng.* 4:377–403.

MacLennan, D. H., and P. T. S. Wong. 1971. Isolation of a calcium sequestering protein from sarcoplasmic reticulum. *Proc. Natl. Acad. Sci. USA.* 68:1231–1235.

Miledi, R., I. Parker, and P. H. Zhu. 1982. Calcium transients evoked by action potentials in frog twitch muscle fibers. *J. Physiol. (Lond.).* 333:655–679.

Mobley, B. A., and B. R. Eisenberg. 1965. Sizes of components in frog skeletal muscle measured by methods of stereology. *J. Gen. Physiol.* 66:31–45.

Neering, I. R., and W. G. Wier. 1980. Kinetics of aequorin luminescence after step changes in calcium concentration: significance for interpretation of intracellular aequorin signals. *Fed. Proc.* 39:1806.

Oetliker, H. 1982. An appraisal of the evidence for a sarcoplasmic reticulum membrane potential and its relation to calcium release in skeletal muscle. *J. Muscle Res. Cell Motil.* 3:247–272.

Ogawa, Y., N. Kurebayashi, A. Irimajiri, and T. Hanai. 1981. Transient kinetics for Ca uptake by fragmented sarcoplasmic reticulum from bullfrog skeletal muscle with reference to the rate of relaxation of living muscle. *Adv. Physiol. Sci.* 5:417–435.

Ostwald, J. J., and D. H. MacLennan. 1974. Isolation of a high affinity calcium binding protein from sarcoplasmic reticulum. *J. Biol. Chem.* 249:974–979.

Peachey, L. D. 1965. The sarcoplasmic reticulum and T-tubules of the frog's sartorius. *J. Cell Biol.* 25:209–231.

Potter, J. D., and J. Gergely. 1975. The calcium and magnesium binding sites on troponin and their role in the regulation of myofibrillar adenosine triphosphatase. *J. Biol. Chem.* 250:4628–4633.

Potter, J. D., and H. G. Zot. 1982. The role of actin in modulating Ca^{2+} binding to troponin. *Biophys. J.* 37(2, Pt. 2):43*a*. (Abstr.)

Reuter, H. 1983. Calcium channel modulated by neurotransmitters, enzymes and drugs. *Nature (Lond.).* 301:569–574.

Robertson, S. P., J. D. Johnson, and J. D. Potter. 1981. The time-course of Ca^{2+} exchange with calmodulin, troponin, parvalbumin, and myosin in response to transient increases in Ca^{2+}. *Biophys. J.* 34:559–569.

Schneider, M. F., and W. K. Chandler. 1973. Voltage-dependent charge movement in skeletal muscle: a possible step in excitation-contraction coupling. *Nature (Lond.).* 242:244–246.

Snowdowne, K. W. 1979. Aequorin luminescence from single fibers at rest. *Fed. Proc.* 38:1443.

Somlyo, A. V., H. Gonzalez-Serratos, H. Schuman, G. McCelland, and A. P. Somlyo. 1981. Calcium release and ionic changes in the sarcoplasmic reticulum of tetanised muscle: an electron probe study. *J. Cell Biol.* 90:577–594.

Sommer, J. R., and E. A. Johnson. 1979. Ultrastructure of cardiac muscle. *In* The Handbook of Physiology. R. M. Berne, editor. The American Physiological Society, Bethesda, MD. 1:113–186.

Stephenson, D. G., I. R. Wendt, and Q. G. Forrest. 1981. Non-uniform ion distributions and electrical potentials in sarcoplasmic regions of skeletal muscle fibers. *Nature (Lond.).* 289:690–692.

Wang, J. H. 1953. Tracer diffusion in liquids. IV. Self-diffusion of calcium ion and chloride ion in aqueous calcium chloride solutions. *J. Am. Chem. Soc.* 75:1769–1770.

Winegrad, S. 1968. Intracellular calcium movements of frog skeletal muscle during recovery from tetanus. *J. Gen. Physiol.* 51:65–83.